α7-nAchR agonist GTS-21 reduces radiation-induced lung injury

ZIJIE MEI[1*], XIAOLI TIAN[2*], JING CHEN[2], YACHENG WANG[2], YE YAO[1], XIN LI[2], CHUNXU YANG[1], SHIMIN ZHANG[2] and CONGHUA XIE[1,2]

[1]Department of Radiation and Medical Oncology, [2]Hubei Key Laboratory of Tumor Biological Behaviors, Zhongnan Hospital, Wuhan University, Wuhan, Hubei 430071, P.R. China

Received January 6, 2018; Accepted July 23, 2018

DOI: 10.3892/or.2018.6616

Abstract. Radiation-induced lung injury (RILI) is a major complication of thoracic radiotherapy that starts as exudative inflammation and proceeds to lung fibrosis, and additional studies are required to develop methods to ameliorate RILI. The aim of this study was to explore whether the nicotinic acetylcholine receptor subtype-7 (α7-nAChR) agonist GTS-21 has a protective effect against RILI. C57BL6 mice were irradiated with 12 Gy to induce a mouse model of RILI. Some of the mice received an i.p. injection of 4 mg/kg GTS-21 for three days with or without radiation treatment. Mice were sacrificed at 1, 3, 7, 14 and 21 days and at 3 and 6 months after irradiation. The results showed that GTS-21 treatment significantly relieved RILI by decreasing TNF-α, IL-1β and IL-6 production in serum via inhibition of NF-κB activation and downregulation of TLR-4 and HMGB1 expression in the lungs. In addition, we found that GTS-21 may regulate the MMP/TIMP balance in RILI. Finally, we found that GTS-21 inhibited NOX-1 and NOX-2 expression, which subsequently reduced ROS levels and Hif-1α expression in RILI. However, GTS-21 showed little effect on lung tissue without radiation exposure. The results above were also validated in RAW264.7 macrophages. Our results showed that activation of the cholinergic anti-inflammatory pathway via the α7-nAChR agonist GTS-21 reduced RILI. The protective effect of GTS-21 against RILI is partly attributed to inhibition of the HMGB1/TLR4/NF-κB pathway and ROS production. Thus, activation of the α7-nAChR pathway may lead to new possibilities in the therapeutic management of RILI.

Correspondence to: Professor Conghua Xie, Department of Radiation and Medical Oncology, Zhongnan Hospital, Wuhan University, 169 Dong Hu Road, Wuhan, Hubei 430071, P.R. China
E-mail: chxie_65@whu.edu.cn

*Contributed equally

Key words: radiation-induced lung injury, α7-nAchR cholinergic anti-inflammatory pathway, GTS-21, HMGB1/TLR-4/NF-κB pathway, ROS, NOX-1/2/4

Introduction

Radiation-induced lung injury (RILI) is the most common and the major obstacle prohibiting the high-dose radiation necessary to eradicate cancer of the thoracic region. Researchers have shown that 13-37% of patients receiving radical radiotherapy for lung cancer will experience lung injury (1). Studies have shown that the main pathophysiological features of RILI are an early phase of acute pneumonitis and a later phase of fibrosis. There are many hypotheses regarding RILI pathogenesis, and the perpetual cascade of cytokine theory is widely accepted (2,3). According to the theory, the response of normal lung tissue to radiation injury is a dynamic and continuous process that involves a variety of cytokines and multiple cell responses.

The proinflammatory cytokines tumour necrosis factor (TNF)-α, interleukin (IL)-1 and IL-6 are likely key mediators in the pathogenesis of radiation pneumonitis. Researchers have shown that TNF-α, IL-6 and IL-1β are all increased in RILI (4). TNF-α is known to induce an acute phase of the inflammatory response and play a role in tissue remodelling (5). TNF-α can stimulate neutrophilic granulocytes to express other cytokines, including IL-1 and IL-6 (6). In addition, TNF-α expression leads to the induction of TGF-β, which is a major pro-fibrotic factor (7). IL-1 and IL-6 are important immune regulatory factors that are involved in the inflammatory response and fibrosis process. Studies have shown that IL-l and IL-6 are circulating cytokine markers for radiation pneumonitis (8).

Macrophages are thought to be the main source of proinflammatory cytokines in the early stages of RILI. Hosoi and colleagues showed that low doses of ionizing radiation in macrophages could induce proinflammatory cytokines such as IL-1β and IL-6 (9). Moreover, a study showed that ionizing radiation led to macrophage-rich pneumonitis, and Johnston and colleagues showed that the cell types predominately recruited to the lung for 24 weeks post-irradiation were macrophages and lymphocytes (10). These results indicate that macrophages play an important role in RILI.

Nuclear factor κB (NF-κB) is a major switch that regulates the body's inflammatory response. In recent studies, ionizing radiation-activated NF-κB was shown to predominantly upregulate genes involved in intercellular communication processes, especially genes encoding cytokines and chemokines, such as IL-1β, IL-6 and TNF-α (11,12). In addition, after

high-dose irradiation, the death and apoptosis of cells such as macrophages can lead to the secretion of high-mobility group protein-1 (HMGB1), which activates NF-κB by binding to Toll-like receptor-4 (TLR4), resulting in the release of proinflammatory cytokines (13). Thus, the HMGB1/TLR4/NF-κB pathway plays an important role in RILI.

The extracellular matrix (ECM) provides physical support to tissues, and ECM remodelling is necessary in RILI. Studies have shown that MMPs and tissue inhibitors of metalloproteinases (TIMPs) are both involved in remodelling the ECM. Yang *et al* showed that MMP-2 and MMP-9 are overexpressed during the inflammatory response to RILI and degrade collagen IV in the basement membrane (14).

In addition to inflammatory factors, oxidative stress and hypoxia also play an important role in RILI. Studies have shown that reactive oxygen species (ROS) can induce DNA damage and initiate a series of repair reactions; these excessive repair responses become the basis of lung injury. Several studies have documented that antioxidants can reduce radiation-induced pulmonary fibrosis. An important molecular source of ROS is the enzyme family of NAD(P)H oxidases (Nox), and the Nox isoforms Nox1, Nox2 and Nox4 have been shown to be involved in pulmonary fibrosis in previous studies (15-17).

Studies of RILI have shown that HIF-1α is activated as early as 4 weeks post-irradiation and is accompanied by enhanced oxidative stress, tissue hypoxia, and NF-κB activity (18). This finding indicates that the NF-κB, ROS and HIF-1α pathways cooperate with each other during irradiation-induced lung injury.

Several researchers have investigated the ways to decrease the extent of RILI, but additional research efforts are still needed (19). Recent studies have revealed an immunomodulatory mechanism to limit inflammatory reactions referred to as the cholinergic anti-inflammatory pathway. This so-called cholinergic anti-inflammatory pathway is mediated by acetylcholine, the principal neurotransmitter of the vagus nerve, through a specific interaction with α7 cholinergic receptors (α7-nAChR) on many cells, such as macrophages, neutrophils, endothelial cells, epithelial cells and lymphocytes. Both electrical stimulation of this pathway (via the vagus nerve) and pharmacological stimulation of peripheral α7-nAChR have been shown to have anti-inflammatory effects on several diseases, such as rheumatoid arthritis (20), mechanical ventilation-induced lung injury (21) and septic acute kidney injury (22).

Although many studies have shown the protective effect of α7-nAChR stimulation in inflammatory diseases, the beneficial role of α7-nAChR in RILI is poorly understood. GTS-21, an agonist of α7-nAChR, was reported to reduce acute lung injury and mechanical ventilation-induced lung injury (21,23). Thus, the aim of this study was to explore whether the α7-nAchR agonist GTS-21 is a radioprotective agent for RILI. In this study, we evaluated the histopathological differences between the GTS-21 and control groups in mouse lungs with or without radiation treatment. Then, we investigated the effect of GTS-21 on TNF-α, IL-1β and IL-6 expression in RILI. Finally, we investigated the influence of GTS-21 on the HMGB1/TLR4/NF-κB pathway and ROS production to demonstrate the mechanisms of reducing RILI.

Materials and methods

Animals. Eight-week-old female C57BL/6J mice (n=120) with an approximate body weight of 20 g were purchased from the Animal Center of Wuhan University (Wuhan, China). The mice, housed 5/cage, were maintained in an environment with 60±5% humidity at 20±1˚C under a 12-h light/dark cycle. All experimental animals were housed under specific-pathogen-free conditions for 1 week prior to the initiation of the experiments. The studies were approved by the Institutional Animal Care and Use Committee (IACUC), Wuhan University, Hubei, China (AUP no. 2013065). All animal experimentation was conducted conforming to the 'Guiding Principles for Research involving Animals and Human Beings' (24).

The mice (n=5 for each time-point per group) were divided into two experimental groups as follows: i) control group, healthy mice that received phosphate-buffered saline (PBS); ii) GTS-21 group, healthy mice that received GTS-21; iii) RT group, healthy mice that received radiation and PBS; and iv) GTS-21+RT group, healthy mice that received both radiation and GTS-21.

Cell culture. Murine RAW264.7 macrophages were obtained from the Cell Resource Center of the Shanghai Institutes for Biological Sciences of the Chinese Academy of Sciences. Cells were cultured in DMEM (GE Healthcare Life Sciences/HyClone Laboratories, Logan, UT, USA) containing 10% fetal bovine serum (FBS; GE Healthcare Life Sciences/HyClone Laboratories) and 1% penicillin/streptomycin solution at 37˚C in a 5% CO_2 atmosphere.

Radiation treatment. For thoracic radiation, mice were anaesthetized by intraperitoneal application of 0.2 ml/20 g chloral hydrate 4% (Melonepharma, Dalian, China) and immobilized by cloth surgical tape. Then, the mice were irradiated with a single dose of 12 Gy from a linear accelerator (Siemens Primus-Hi, Munich, Germany). This dose was considered a regular dose to elicit a response from lung disease (26). The beam was 6-MV photons at a dose rate of 1.886 Gy/min, the source-surface distance (SSD) was 100 cm, and the radiation field (2.5x15 cm) was set to cover the whole lung. After radiation, the mice were maintained in a specific-pathogen-free environment and provided a standard diet and water.

α7-nAchR agonist GTS-21. GTS-21 was purchased from Abcam (Cambridge, UK) as a powder, diluted with sterilized water to a final concentration of 500 μg/ml, and then stored at 4˚C. Mice received an i.p. injection of 4 mg/kg GTS-21 (160 μl) or 160 μl of PBS daily for three days with or without radiation. The dose was based on early studies that demonstrated that the anti-inflammatory effects of GTS-21 in mice were dose dependent and that 4 mg/kg GTS-21 significantly attenuated cytokine production (26,27). Furthermore, 4 mg/kg GTS-21 is a non-toxic dose according to the manufacturer's instructions. GTS-21 was also diluted to different concentrations (0, 10, 100, 1,000 and 10,000 nM) for RAW264.7 cell treatment.

Tissue isolation. Mice in the GTS-21 and control groups were sacrificed by cervical dislocation on days 1, 3 and 7 after GTS-21 treatment. Mice in the RT control and GTS-21+RT

groups were sacrificed by cervical dislocation before irradiation (day 0) and at 1, 3, 7, 14 and 21 days and at 3 and 6 months post-irradiation. The left lung lobes were excised for histopathology analyses and measurement of hydroxyproline content. The right lung lobes were snap-frozen in liquid nitrogen and later used for RNA and protein isolation. Serum samples were analyzed using a Cytometric Bead Array (CBA) kit (Becton Dickinson and Company, Franklin Lakes, NJ, USA).

Histopathological analysis. Histological analysis of mouse tissues was performed systematically at every time point after irradiation until 6 months, as previously described. In brief, parts of the left lung were fixed with 4% formalin for 24 h and paraffin embedded. Sections of 4 μm thickness were cut and stained with haematoxylin and eosin (H&E) to determine the inflammation level and stained with Masson's trichrome to detect collagen deposition. The fibrosis score was quantified in a blinded manner by 2 independent investigators using light microscopy, according to the criteria of Hübner *et al* (28). The hydroxyproline content was detected by an alkaline hydrolysis assay kit (Jiancheng Biological Institution, Nanjing, China) that can indirectly examine collagen content in the lungs. According to the manufacturer's instructions, the calculation method for hydroxyproline content was as follows: Content of hydroxyproline (μg/mg, wet weight) = [absorbance (sample) - absorbance (blank)]/[absorbance (standard) - absorbance (blank)] x 5 μg/ml x 10 ml/weight (tissue).

Real-time PCR. Total RNA was extracted from lung tissue or cells with Invitrogen™ TRIzol reagent (Thermo Fisher Scientific, Inc., Waltham, MA, USA) according to the manufacturer's protocol. cDNA was synthesized from 5 μg of total RNA following the manufacturer's instructions (RevertAid RT kit; Thermo Fisher Scientific, Inc.). Quantification was performed with SYBR Premix Ex Taq™ (Takara Bio Inc., Shiga, Japan) in a 20 ml reaction volume. The following primers were used to amplify TLR-4, HMGB1 and MyD88: TLR-4 (forward primer, 5'-AGTTTAGAGAATCTGGTGGCT GTG-3' and reverse primer, 5'-TTCCCTGAAAGGCTTGGT CT-3'); HMGB1 (forward primer, 5'-ACAGCCATTGCAGTA CATTGAG-3' and reverse primer, 5'-TGCCCATGTTTAGTT GATTTCCC-3'); and MyD88 (forward primer, 5'-CCAGCG AGCTAATTGAGAAAAG-3' and reverse primer, 5'-ATAGTG ATGAACCGCAGGATAC-3'). Data analyses were performed using the $2^{-\Delta\Delta Cq}$ method (29).

Western blot analysis. After protein isolation and homogenization of the frozen mouse lung, the protein content was determined, and equal amounts of protein (50 μg/condition) were separated by SDS-PAGE and transferred to a PVDF membrane (Millipore, Billerica, MA, USA) for western blotting. The non-specific sites were blocked in 5% non-fat dry milk at room temperature for 1 h. In this study, antibodies directed against MyD88 (1:500; cat. no. 66660-1-l g; Proteintech Group, Chicago, IL, USA), MMP2 (1:500; cat. no. 66366-1-l g; Proteintech Group), MMP-9 (1:500; cat. no. 10375-2-AP; Proteintech Group), HIF-1α (1:1,000; cat. no. ab187524; Abcam), TLR-4 (1:1,000; cat. no. ab13556; Abcam), HMGB1 (1:1,000; cat. no. ab79823; Abcam) and TIMP1 (1:1,000; cat. no. ab86482; Abcam) were used. The secondary antibodies were goat anti-mouse horseradish peroxidase antibody (cat. no. 1706516; Bio-Rad Laboratories, Inc., Hercules, CA, USA) or goat anti-rabbit horseradish peroxidase antibody (cat. no. 1662408; Bio-Rad Laboratories, Inc.) used at 1:20,000 or 1:10,000, respectively.

Immunohistochemistry. Slides were deparaffinized, rehydrated though a graded series of ethanol and treated with 3% H_2O_2 in H_2O to quench endogenous peroxidase activity. The specimens were incubated overnight at 4˚C with 100-fold diluted rabbit polyclonal antibody against NF-κB p65 (1:100; cat. no. 10745-1-AP; Proteintech Group) and goat anti-rabbit secondary antibody (1:50; cat. no. a0208; Beyotime Institute of Biotechnology, Haimen, China); diaminobenzidine (DAB) was then used as the chromogen.

Dihydroethidium (DHE) ROS detection assay. Unfixed frozen lung tissues were cut into 8-μm sections and placed on glass slides. Slides were incubated with 1 μM dihydroethidium (DHE) in a light-protected, humidified chamber at 37˚C for 30 min, and then coverslipped. Tissue sections were then visualized with an Olympus BX53 fluorescence microscope (Olympus Corp., Tokyo, Japan), and fluorescence was detected with a 590 nm long-pass filter. Images were collected and stored digitally.

RAW246.7 cells were seeded at $5x10^5$ cells/well in 6-well plates. After cultivation overnight, cells were treated with or without GTS-21 (100 nM) after 6 Gy irradiation. After 24 h of cultivation, cells were incubated with 1 μM dihydroethidium (DHE) and placed in a chamber at 37˚C for 30 min.

Serum cytokine measurements. Murine serum was collected from euthanized mice at every time point post-irradiation. TNF-α, IL-1β and IL-6 in serum from mice were determined using a CBA kit (BD Biosciences, San Diego, CA, USA) according to the manufacturer's instructions.

MTT assays. RAW264.7 cells in the exponential growth phase were seeded at a density of 5,000 cells/well in 96-well plates and irradiated with 6 Gy. Then, the cells were treated with 200 μl of 0, 10, 100, 1,000 and 10,000 nM GTS-21 and cultured for 24, 48, 72, 96 and 120 h at 37˚C in a humidified 5% CO_2 incubator. MTT assays were performed according to the manufacturer's instructions (Beyotime Institute of Technology, Nanjing, China). The absorbance values were determined at 570 nm on a Moduluse II Microplate Multimode Reader (Turner BioSystems Inc., Sunnyvale, CA, USA). All MTT assays were performed three times in quintuplicate.

Statistical analyses. The data are presented as the mean ± SEM. The data for the various time points were analyzed by one-way ANOVA and unpaired two-tailed t-tests. Multiple comparisons between the groups were performed using Tukey's post hoc test. $P<0.05$ were considered statistically significant.

Results

GTS-21 reduces lung inflammatory infiltrate and fibrosis in radiation-treated mice. Based on the results of H&E staining, GTS-21 treatment had little effect on lung tissue in the absence

of irradiation (Fig. 1A). Meanwhile, radiation treatment of mice without GTS-21 treatment increased the inflammatory response in the lungs over time, with the most notable response at 21 days after radiation treatment. In contrast, the GTS-21+RT group showed significantly lower inflammation on day 21 (Fig. 1B). Histological evaluation revealed that the fibrosis level was significantly decreased in the GTS-21+RT group compared with the RT control after 6 months but was not significantly different between the GTS-21 and RT control groups (Fig. 1C and D). To more accurately evaluate the fibrosis level among the four groups, we quantified lung fibrosis levels using a modified Ashcroft scale based on hydroxyproline content. The fibrosis score was significantly decreased in the GTS-21 treatment group compared with the RT control group at 6 months after irradiation (3±0.63 and 4.8±0.44, respectively, P=0.001), while the RT control and GTS-21 groups showed no difference in the effect at 3 or 6 months (Fig. 1E). We then used hydroxyproline to test the fibrosis level of the lung in the four groups at 6 months after irradiation. The results showed that the hydroxyproline levels in the control and GTS-21 groups were not different after 6 months. However, we observed significantly lower expression of hydroxyproline in the GTS-21+RT group than in the RT control group at 6 months (0.72±0.06 and 0.97±0.17 μg/mg, respectively, P=0.03; Fig. 1F).

GTS-21 reduces the levels of TNF-α, IL-1β and IL-6 in radiation-treated mice. To assess the inflammatory cytokine response to GTS-21 treatment with or without radiation treatment, we measured three specific proinflammatory cytokines (TNF-α, IL-1β and IL-6) in the mouse sera. The results showed that TNF-α expression was significantly decreased in the GTS-21+RT group compared to the RT control group, especially at 21 days post-radiation (Fig. 2A). IL-1β expression was also lower in the GTS-21+RT group than in the RT control group at 21 days after irradiation, and it remained significantly lower at 3 and 6 months post-radiation. However, we found no significant difference in IL-1β expression between the GTS-21+RT group and RT control group during the early stages of the inflammatory response (Fig. 2B). Fig. 2C shows that the level of IL-6 in the GTS-21+RT group was significantly decreased at 14 and 21 days and 3 months after irradiation, while there was no significant difference at other time points. Furthermore, we found that the levels of TNF-α, IL-1β and IL-6 were not different between the control and GTS-21 groups, indicating that GTS-21 had little effect on proinflammatory cytokines without irradiation.

GTS-21 inhibits the HMGB1/TLR-4/NF-κB pathway and regulates MMP/TIMP balance after irradiation. Since the NF-κB heterodimer p50/p65 is most often activated in the radiation response and only p65 contains the transactivation domain in its C-terminal region, the activity of NF-κB can be evaluated by detecting the expression of p65. In this study, we performed immunohistochemistry to detect NF-κB p65 expression in the GTS-21+RT and RT groups at the inflammatory stage after irradiation (Fig. 3A). The results showed that NF-κB p65 was significantly inhibited at 21 days in the GTS-21+RT group compared with the RT control. Then, we compared the mRNA expression levels of TLR-4, HMGB1 and MyD88 in the RT and GTS-21+RT groups at the inflammatory response stage. As shown in Fig. 3B, the mRNA level of TLR-4 in the GTS-21 treatment group trended towards an increase at 1 day after irradiation compared with the control, but was rapidly decreased in the following days after irradiation. The most significant fold change was revealed at 21 days post-radiation (GTS-21+RT compared to RT control, 0.25±0.11, P≤0.05). HMGB1 mRNA expression was immediately decreased after irradiation in the GTS-21 treatment group compared with the RT control group (GTS-21+RT compared to RT control, 0.31±0.15, P≤0.05) and continued to decrease at the following time points, especially at 21 days post-radiation (GTS-21+RT compared to RT control, 0.27±0.10, P≤0.05). However, we did not find any differences in HMGB1 expression between the two groups at 7 days post-radiation (Fig. 3C). Then, we examined the mRNA level of MyD88 in the GTS-21+RT and RT control groups, but no difference was found between them (Fig. 3D). Because the inflammatory response was significantly different between the two groups on day 21 post-radiation, we chose the time point of day 21 post-radiation to confirm the effect of GTS-21 on the protein levels of TLR-4, HMGB1 and MyD88. The results showed that TLR-4 and HMGB1 protein expression was significantly reduced in mice treated with GTS-21. However, we did not observe any alteration in the protein level of MyD88 (Fig. 3E). Furthermore, to elucidate the effect of GTS-21 on extracellular matrix metalloproteinases that are commonly involved in RILI, we examined their protein levels on day 21 and at 6 months after irradiation. The results showed that MMP-2 and MMP-9 protein expression was significantly reduced in GTS-21-treated mice on day 21 and increased at 6 months after irradiation compared with RT control mice. TIMP-1 was increased on day 21 and decreased at 6 months after irradiation in the GTS-21 treatment group compared to the RT control group (Fig. 3F).

GTS-21 alleviates tissue hypoxia and reduces ROS levels by inhibiting NOX-1 and NOX-2 in radiation pneumonitis. To elucidate the effect of GTS-21 on ROS production in radiation pneumonitis, we used DHE to analyze ROS in mouse lungs on day 21 after irradiation. The results revealed that the ROS level in lung tissues from the GTS-21+RT treatment group was significantly reduced at 21 days after irradiation compared to that from the RT control group. However, we did not observe any difference in the GTS-21 and control groups without irradiation (Fig. 4A). To further clarify the relevant mechanisms, real-time PCR was used to detect the mRNA levels of NOX1/2/4 in the GTS-21+RT and RT groups. The results showed that the mRNA level of NOX-1 was reduced significantly in the GTS-21 treatment group, except on day 7 after irradiation (P<0.05); NOX-2 mRNA expression was also inhibited in the GTS-21+RT group, especially at 21 days post-irradiation. There was no difference in NOX-4 expression between the GTS-21+RT and RT groups (Fig. 4B). Fig. 4C shows the corresponding NOX protein levels on day 21 after irradiation in GTS-21-treated mice and control mice, as evaluated by western blot analysis. Finally, we found that the protein level of HIF-1α was significantly reduced at 14 and 21 days after irradiation in the GTS-21+RT group compared to the RT control (Fig. 4D).

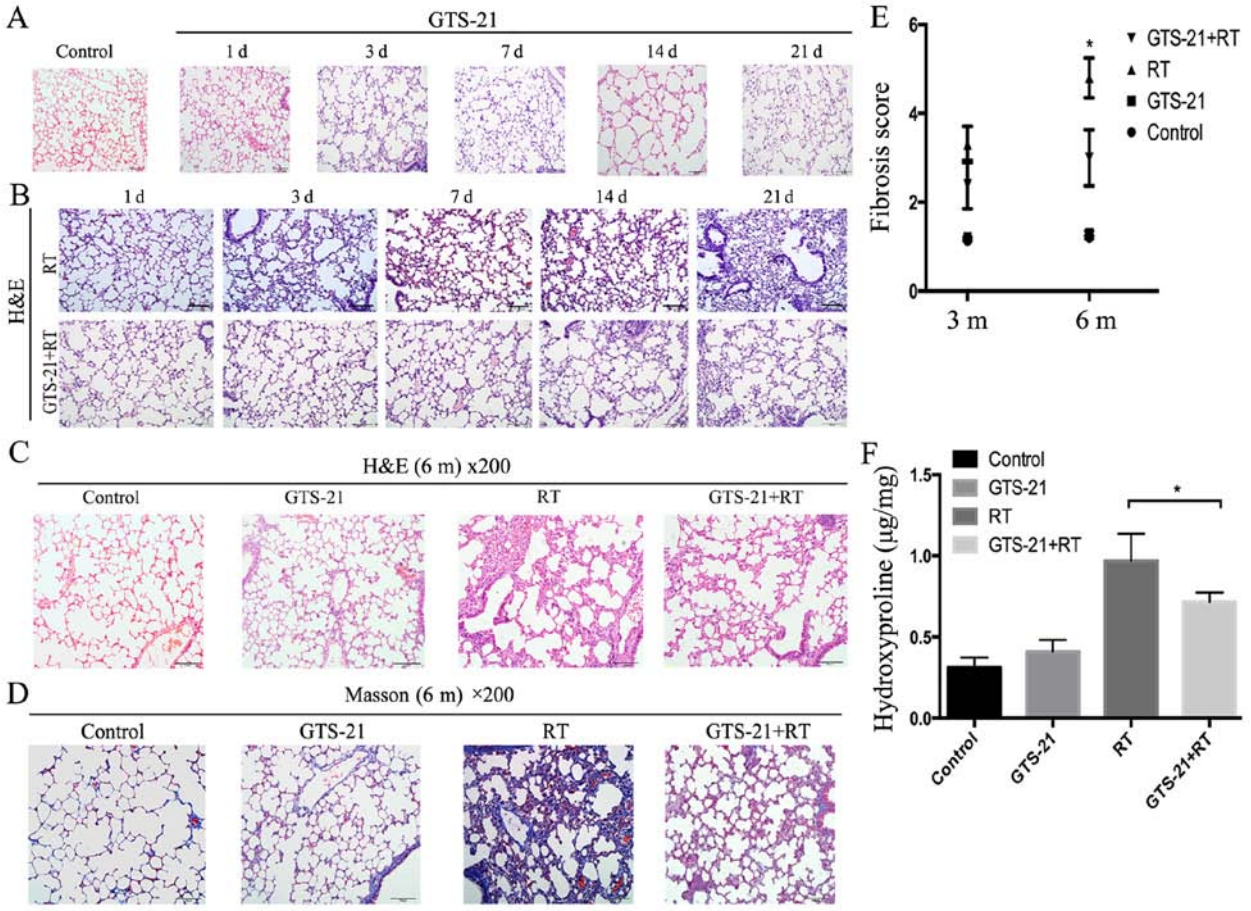

Figure 1. GTS-21 reduces radiation-induced histological signs of pulmonary injury. (A) Lungs were removed on days (d) 1, 3, 7, 14 and 21 after GTS-21 or PBS treatment and stained with haematoxylin and eosin (H&E). (B) Lungs were removed at the indicated times after RT or GTS-21+RT and stained with H&E to assess the extent of inflammation and fibrosis. (C and D) H&E-stained and Masson's trichrome-stained sections viewed at x200 magnification at 6 months (m) after the following treatments: PBS administration, GTS-21 administration, irradiation or GTS-21 administration and irradiation treatment combined with GTS-21 administration. (E) The fibrosis scores were calculated for the four groups (control, GTS-21, RT and GTS-21+RT) at different time-points. (F) The hydroxyproline content was detected in the lungs removed from mice after PBS, GTS-21, radiation or GTS-21 and radiation combination treatment for 6 months. Error bars represent the SEM. *P<0.05. Groups: Control, healthy mice that received phosphate-buffered saline (PBS); GTS-21, healthy mice that received GTS-21; RT, healthy mice that received radiation and PBS; and GTS-21+RT, healthy mice that received both radiation and GTS-21.

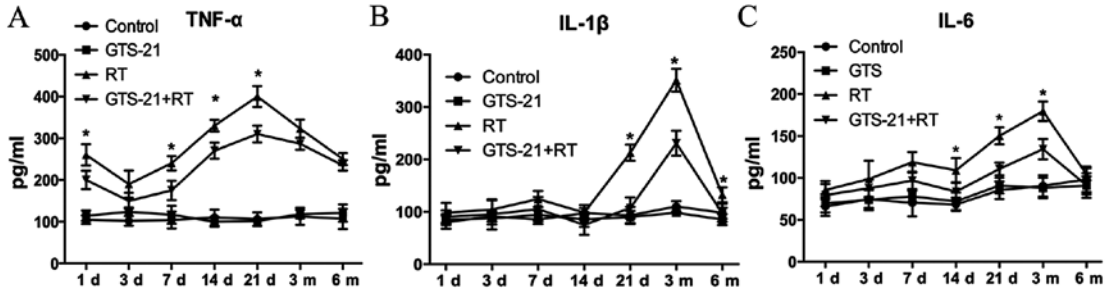

Figure 2. GTS-21 reduces inflammatory cytokine production after irradiation. Cytokine production in the control, GTS-21, RT and GTS-21+RT groups was evaluated using a CBA kit. (A) TNF-α; (B) IL-1ß; and (C) IL-6. Error bars represent the SEM. *P<0.05. Groups: Control, healthy mice that received phosphate-buffered saline (PBS); GTS-21, healthy mice that received GTS-21; RT, healthy mice that received radiation and PBS; and GTS-21+RT, healthy mice that received both radiation and GTS-21. m, months; d, days.

GTS-21 suppresses cell proliferation and inhibits the HMGB1/TLR-4/NF-κB pathway and ROS production in RAW264.7 cells after irradiation. Macrophages are the most active cells in lung tissue, and they are considered to be the main source of inflammatory cytokines in lung tissue after irradiation. Here, we used murine RAW264.7 macrophages to confirm the effect of GTS-21 on the inflammatory response *in vitro*. First, we used MTT assays to detect whether GTS-21 can influence RAW264.7 cell proliferation, and the result showed that RAW264.7 cell proliferation was significantly inhibited with both low-dose (10 and 100 nM) and high-dose (1,000 and 10,000 nM) GTS-21 (Fig. 5A). Then, cells were treated with three doses of GTS-21 immediately after irradiation, and the mRNA levels of TLR-4, HMGB1, and MyD88 were examined

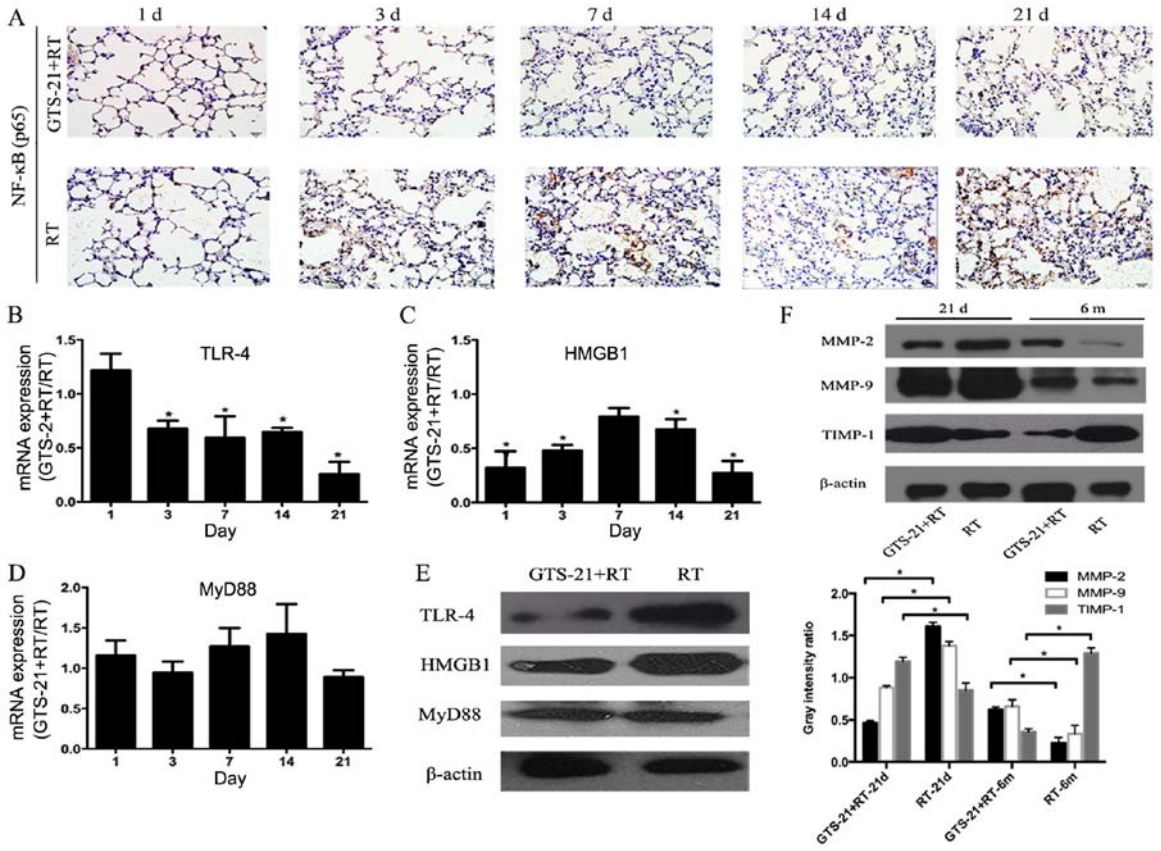

Figure 3. GTS-21 inhibits the HMGB1/TLR-4/NF-κB pathway and MMP/TIMP balance after irradiation. (A) The protein level of NF-κB (p65) was detected using immunohistochemical analysis at the inflammatory stage after irradiation. Magnification, x400. Representative real-time RT-PCR analysis of TLR4 (B), HMGB1 (C) and MyD88 (D) at the indicated times after irradiation with or without GTS-21 treatment. (E) The protein levels of TLR-4, HMGB1 and MyD88 were detected on day 21 post-radiation in the GTS-21+RT and RT groups. (F) The protein levels of MMP-2, MMP-9 and TIMP-1 were examined at 21 days (21 d) and 6 months (6 m) after irradiation (RT) with or without GTS-21 treatment. The gray intensity ratio was calculated using ImageJ Software v1.8.0 (National Institutes of Health, Bethesda, MD, USA). Each gray value was detected three times. Error bars represent the SEM. *P<0.05.

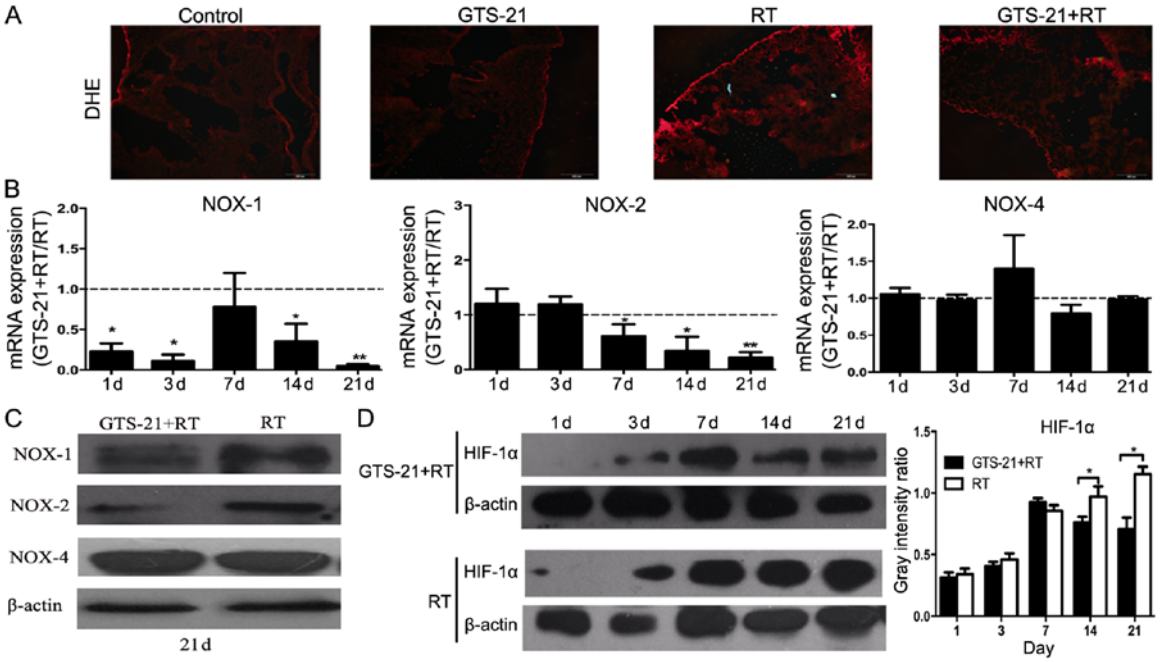

Figure 4. GTS-21 inhibits ROS production, NOX1/2/4 expression and HIF-1α expression at the inflammation stage after irradiation. (A) Representative images of DHE staining in the lungs. The different experimental conditions are indicated at the top of each image. Magnification, x100. (B) Real-time PCR was performed to measure NOX-1/2/4 expression from day 1 (1 d) to day 21 (21 d) after irradiation (RT) with or without GTS-21 stimulation. (C) Western blot analysis of corresponding NOX protein levels on day 21 after irradiation. ß-actin was used as a loading control. (D) HIF-1α protein levels were detected at the inflammation stage in the GTS-21+RT and RT control groups. The gray intensity ratio was calculated using ImageJ software. Each gray value was detected three times. Error bars represent the SEM. *P<0.05. Groups: Control, healthy mice that received phosphate-buffered saline (PBS); GTS-21, healthy mice that received GTS-21; RT, healthy mice that received radiation and PBS; and GTS-21+RT, healthy mice that received both radiation and GTS-21.

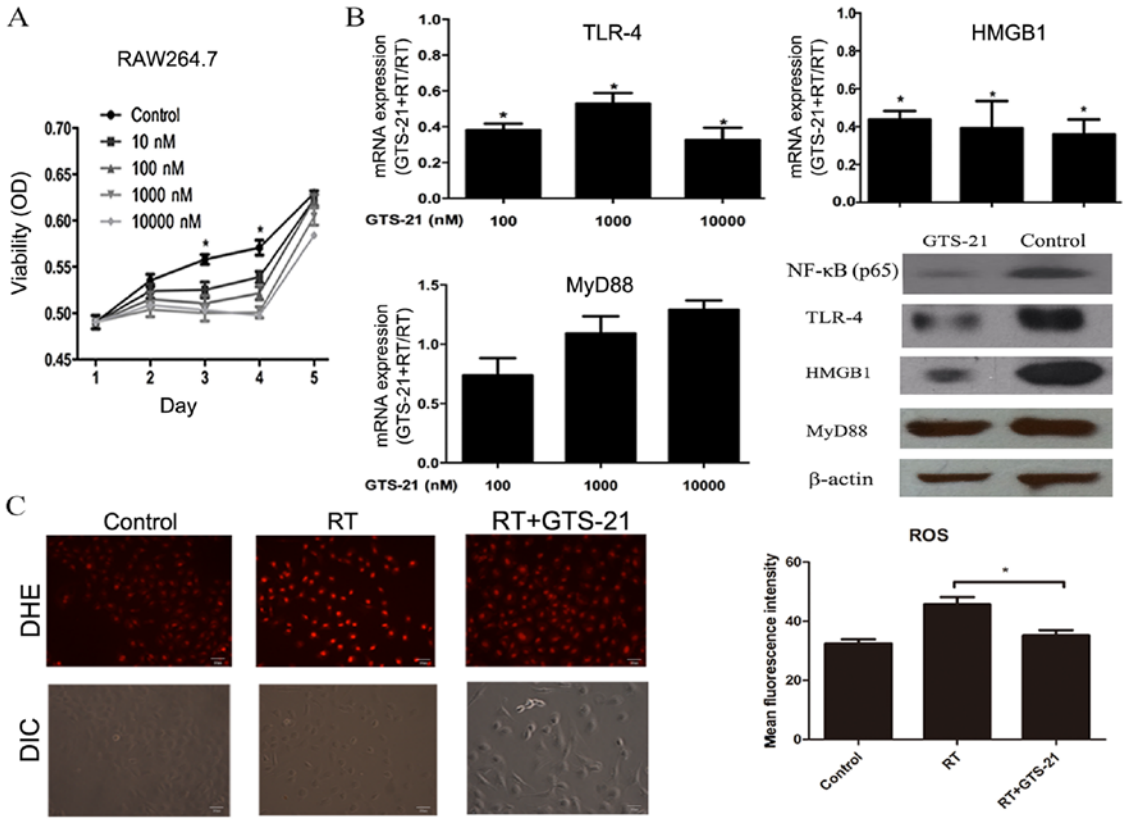

Figure 5. Effect of GTS-21 on RAW264.7 macrophages after irradiation. (A) RAW264.7 cells were irradiated at 6 Gy and treated with different concentrations of GTS-21 (0, 10, 100, 1,000 and 10,000 nM) after irradiation. After 1, 2, 3, 4 and 5 days, the cells were subjected to MTT assays. (B) RAW264.7 cells were irradiated at 6 Gy and treated with or without GTS-21 (100, 1,000 and 10,000 nM). After 48 h, the mRNA levels of HMGB1, TLR4 and MyD88 were analyzed by real-time PCR. The protein levels of NF-κB (p65), TLR4, HMGB1 and MyD88 were detected in cells that were treated with or without GTS-21 (100 nM) at 48 h after irradiation. (C) RAW264.7 cells were irradiated at 6 Gy and treated with or without GTS-21 (100 nM). Unirradiated cells were used as negative controls. After 24 h, ROS production in each group was observed by DHE. Statistical data of fluorescence measurements are presented as histograms (right). Magnification, x200. Error bars represent the SEM. *P<0.05. Groups: Control, healthy mice that received phosphate-buffered saline (PBS); GTS-21, healthy mice that received GTS-21; RT, healthy mice that received radiation and PBS; and GTS-21+RT, healthy mice that received both radiation and GTS-21.

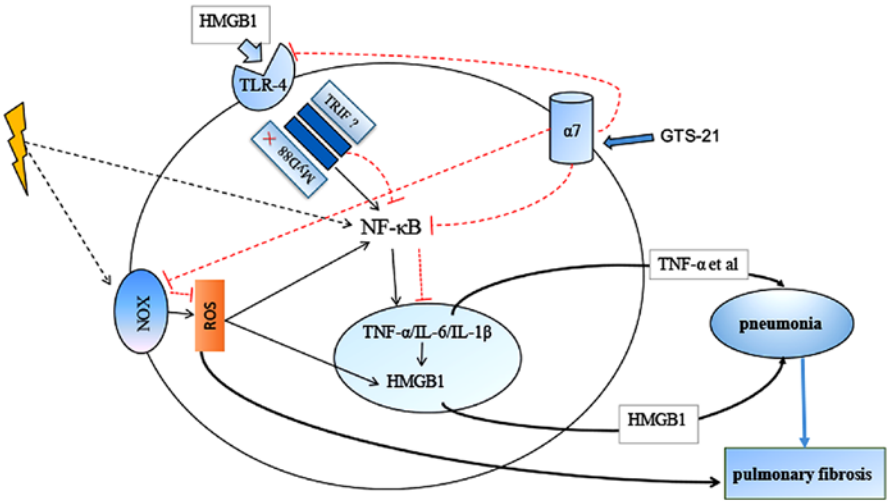

Figure 6. Mechanism of GTS-21 protective role in radiation-induced lung injury. After high-dose irradiation, the death and apoptosis of cells such as macrophages can lead to the secretion of high-mobility group protein-1 (HMGB1), which activates TLR-4, subsequently activating NF-KB through MyD88 or MyD88-independent pathway and resulting in the release of proinflammatory cytokines such as TNF-α, IL-1β and IL-6. These proinflammatory cytokines can also upregulate HMGB1, forming a positive feedback loop that continues to promote inflammatory signalling. GTS-21, an agonist of α7-nAChR, can inhibit TLR-4 through MyD88-independent pathway and inhibit HMGB1expresstions which following inhibits NF-KB activation. Second, ROS can activate NF-κB immediately and act as the initiating factor of early inflammation after irradiation. GTS-21 reduced the expression of NOX-1/2 and, thus, reduced radiation-induced ROS generation.

by real-time PCR. The results showed that each dose could significantly reduce the mRNA levels of HMGB1 and TLR-4 but not MyD88, which was consistent with the experimental data obtained *in vivo*. Since 100 nM GTS-21 was sufficient to

achieve the desired effect, we next used 100 nM GTS-21 to confirm its effect on the protein levels of NF-κB(p65), TLR-4, HMGB1 and MyD88. The results showed that the protein levels of NF-κB(p65), HMGB1 and TLR-4 in RAW264.7 cells were also significantly reduced after GTS-21 treatment. Similarly, there was no significant change in the expression of MyD88 between the GTS-21+RT and RT groups (Fig. 5B). Finally, we confirmed the effect of GTS-21 on ROS production in RAW264.7 cells after irradiation, and DHE staining revealed that the ROS level was significantly decreased in the GTS-21 group after 6 Gy irradiation when compared to the RT only group (Fig. 5C).

Discussion

Radiation-induced pneumonia and fibrosis often occur as a complication of thoracic irradiation, which leads to reduced radiation treatment doses and, subsequently, decreased efficiency against cancer. However, there is a lack of effective therapies to prevent this severe side-effect, which requires further study.

Our results demonstrated that stimulation of the vagus nerve through the α7-nAChR agonist GTS-21 markedly reduced the extent and severity of radiation-induced pneumonia and fibrosis in mice. Moreover, the levels of proinflammatory cytokines such as TNF-α, IL-1β and IL-6 were all reduced in mice treated with GTS-21 after irradiation. Finally, we demonstrated that the protective effect of GTS-21 on RILI occurred partly through inhibition of the HMGB1/TLR4/NF-κB pathway and ROS production. The results were verified *in vitro*.

GTS-21 is a selective agonist of α7-nAChR with anti-inflammatory and cognition-enhancing activities. In two phase II clinical trials, volunteers were observed to have good tolerance to GTS-21 (30,31). In the present study, we used the recommended dose (4 mg/kg) of GTS-21 in mice after irradiation, which resulted in decreased inflammatory infiltrate and subsequently alleviated late fibrosis according to a histopathological analysis. Similar results were shown by Leib and colleagues, who showed that activation of the cholinergic pathway through α7-nAChR could reduce inflammation and fibrosis in the myocardium (32).

TNF-α, IL-1β and IL-6 have been shown to play a role in the pathogenesis of RILI. Moreover, the results from previous studies have shown that inhibiting TNF-α and IL-6 could reduce radiation-induced lung fibrosis (33,34). In addition, research from Zhao and colleagues showed that standardized Myrtol could attenuate RILI by inhibiting TNF-α, IL-1β and IL-6 expression (35). Thus, inhibition of these proinflammatory cytokines may protect against the development of RILI in mice. In the present study, we showed that the agonist α7-nAChR led to reduced secretion of TNF-α immediately after irradiation, and the most obvious difference was observed at 21 days post-radiation. Furthermore, despite the low expression of IL-6 and IL-1β observed in the GTS-21+RT group, the differences in expression between the GTS-21+RT and RT groups were observed only after 14 days. Rübe *et al* showed that IL-6 and IL-1 expression was maintained at a low level during the early inflammatory response and increased at 4 weeks after irradiation (36). Therefore, we concluded that the expression of IL-6 and IL-1β may be low at early time points after irradiation, making it difficult to detect differences between groups.

NF-κB is a master switch in inflammation and the central element of the acute innate immune response. Studies have shown that NF-κB is immediately activated after exposure to radiation and subsequently upregulates inflammatory cytokines, chemokines and apoptosis-related factors, which promote inflammation in tissue (11). Haase and colleagues showed that NF-κB activation was sustained throughout the progression of RILI in rats (37). Here, we showed that GTS-21 treatment reduced the protein level of NF-κB(p65) during the early stage of inflammation and clearly inhibited its expression on day 21 after irradiation, which was the most severe period of the inflammatory response, in the RT control group. The results indicate that GTS-21 can reduce radiation pneumonitis by inhibiting the activation of NF-κB. Li and colleagues demonstrated that α7-nAChR agonists could protect the liver from ischaemia-reperfusion injury by inhibiting the expression of NF-κB(p65), which is consistent with the results of our study (39). Café-Mendes and colleagues also showed that α7-nAChR agonists decreased LPS-induced activation of NF-κB in the neuroinflammatory system of the hippocampus (40).

Toll-like receptor (TLR)-4 is an innate immune receptor expressed by macrophages, dendritic cells, lymphocytes and other immune cells (41). TLR-4 can recognize endogenous ligands released by damaged or stressed tissues, including HMGB1 (41). This triggers downstream signaling cascades in a bifurcated fashion via MyD88 and TRIF. A recent study showed that knockout of TLR-4 in C57BL/6 mice significantly reduced radiation-induced pulmonary fibrosis (42). In the present study, we found that GTS-21 reduced TLR-4 transcript and protein levels in mouse lungs compared with those in control lungs. This result was consistent with that from a study by Kox *et al* which showed that GTS-21 downregulated the monocyte cell-surface expression of TLR4 during inflammation (43). However, we found that the expression of MyD88 did not differ between the GTS-21+RT and RT groups after irradiation, which indicated that GTS-21 had no effect on the MyD88 signaling pathway.

HMGB1 is present in all eukaryotic cells as a conserved nuclear protein, and it can be secreted by the cell in response to lipopolysaccharide, IL-1 or TNF-α stimulation. Moreover, HMGB1 can bind to TLR-4 and activate NF-κB inflammatory signaling pathways, which promote inflammatory cytokine release (44-46). Studies have shown that radiation can directly stimulate cells to secrete HMGB1 and increase the expression of TLR-4 through a p53-dependent pathway (47,48). Furthermore, as mentioned above, the HMGB1/TLR-4/NF-κB pathway can be activated directly by radiation, which promotes an inflammatory reaction. However, in this study, we found that the α7-nAChR agonist GTS-21 reduced the transcript level of HMGB1 at the early stage of inflammation and notably inhibited its expression on day 21 post-radiation. The protein level of HMGB1 on day 21 was also decreased in the GTS-21 group. Sitapara and colleagues demonstrated that GTS-21 effectively protected against mechanical ventilation-induced lung injury by inhibiting HMGB1 release from macrophages, which is consistent with the results of this study (23).

The proteolytic activity of the MMPs is related to extracellular matrix degradation, and it is precisely regulated by TIMPs in tissue. Disruption of this balance is usually observed in RILI. Li and colleagues showed that MMP inhibitors prevented irradiation-induced lung injury in mice (49). In this study, we investigated whether GTS-21 stimulation had an effect on extracellular MMPs and TIMPs. Here, we showed that GTS-21 treatment reduced MMP-2/9 protein levels and increased TIMP-1 levels at the pulmonary inflammation stage after irradiation. We further observed that MMP-2/9 expression levels were higher while TIMP-1 expression levels were lower in the GTS-21 treatment group than in the RT control group during the pulmonary fibrosis stage. These results indicated that GTS-21 may regulate the MMP/TIMP balance in RILI.

ROS can immediately activate NF-κB and act as the initiating factor of early inflammation after irradiation. Thus, to investigate the effect of GTS-21 on ROS production in mouse lung tissue after irradiation, we used DHE to detect ROS levels in the lung tissue of GTS-21-treated and control mice at 21 days after irradiation. We found that GTS-21 reduced ROS production on day 21 after irradiation compared to that in the controls. Studies by Hiramoto *et al* (50) and Navarro *et al* (51) showed that α7-nAchR agonists could reduce the level of ROS, which is similar to our findings.

NADPH oxidase is one of the major sources of ROS generation. It is a multi-protein complex enzyme that is functionally expressed in many cells. Recent studies have indicated that NADPH oxidase-derived ROS play a pathophysiological role in radiation-induced normal tissue injury (52). NOX-1/2/4 are the most widely studied subunits in the present study. To further clarify the possible mechanism by which GTS-21 inhibits ROS, we detected the expression of NOX-1/2/4 in the lung tissues of the GTS-21+RT and RT groups after irradiation. The results showed that GTS-21 could reduce the expression of NOX-1/2 but had no effect on the expression of NOX-4.

HIF-1α is closely related to radiation pneumonitis and pulmonary fibrosis in mice. Researchers have speculated that HIF-1α inhibitors may have protective effects on RILI. The present study examined the expression of HIF-1α in lung tissue after 1, 3, 7, 14 and 21 days in the GTS-21-treated and control groups after irradiation. The results showed that the expression of HIF-1α in the GTS-21+RT group was lower than that in the control group 14 days post-radiation. The results indicated that GTS-21 could reduce the expression of HIF-1α in lung tissue after irradiation. Since GTS-21 and HIF-1α have not been demonstrated by any study to directly interact, the reduction of HIF-1α may depend on the improvement of the inflammatory environment, reduction of ROS production and decrease in the degree of pulmonary fibrosis by GTS-21.

Based on the results above, we found that GTS-21 inhibited the HMGB1/TLR-4/NF-κB pathway and reduced ROS production in the RILI mouse model. The mechanism of GTS-21 in RILI is shown in Fig. 6. As macrophages are considered to be very important target cells in RILI and highly express α7-nAchR, we further confirmed the effect of GTS-21 on macrophages after irradiation. Our results showed that GTS-21 inhibited macrophage proliferation after irradiation. Jenkins and colleagues found that local macrophage proliferation rather than recruitment from the blood was a feature of Th2 inflammation (53). Moreover, a previous study from our group showed that RILI was also the result of a Th2-like immune response (54). Thus, we hypothesized that GTS-21 may alleviate RILI by inhibiting macrophage proliferation. We found that GTS-21 could inhibit NF-κB activation and suppress the expression of HMGB1 and TLR-4 transcripts and protein after irradiation, although it had no effect on MyD88 expression. These results were consistent with the *in vivo* results, which indicated that GTS-21 could reduce RILI by inhibiting the HMGB1/TLR-4/NF-κB inflammatory pathway in macrophages. Finally, we examined ROS production in macrophages after irradiation with or without GTS-21 treatment, and the results showed that GTS-21 also reduced ROS production in macrophages after irradiation.

Acknowledgements

Not applicable.

Funding

The present study was supported by the National Natural Science Foundation of China (grant no. 81272996) and the Natural Science Foundation of Hubei Province (grant no. 2013CFA006).

Availability of data and materials

The datasets used during the present study are available from the corresponding author upon reasonable request.

Authors' contributions

ZM and XT carried out most of the practical work and drafted the manuscript. JC and YW contributed to the analysis and interpretation of the data. YY and XL performed the animal experiment. CY and SZ performed part of the molecular biology and cell culture. CX participated in the study design and modified the manuscript. All authors read and approved the manuscript and agree to be accountable for all aspects of the research in ensuring that the accuracy or integrity of any part of the work are appropriately investigated and resolved.

Ethics approval and consent to participate

The studies were approved by the Institutional Animal Care and Use Committee (IACUC), Wuhan University, Hubei, China (AUP no. 2013065).

Patient consent for publication

Not applicable.

Competing interests

The authors declare that they have no competing interests.

Authors' information

Part of this work was presented as a poster at the IASLC 17th World Conference on Lung Cancer (55).

References

1. Das SK, Zhou S, Zhang J, Yin FF, Dewhirst MW and Marks LB: Predicting lung radiotherapy-induced pneumonitis using a model combining parametric Lyman probit with nonparametric decision trees. Int J Radiat Oncol Biol Phys 68: 1212-1221, 2007.
2. Pahl HL: Activators and target genes of Rel/NF-kappaB transcription factors. Oncogene 18: 6853-6866, 1999.
3. Iademarco MF, McQuillan JJ, Rosen GD and Dean DC: Characterization of the promoter for vascular cell adhesion molecule-1 (VCAM-1). J Biol Chem 267: 16323-16329, 1992.
4. Liu GD, Xia L, Zhu JW, Ou S, Li MX, He Y, Luo W, Li J, Zhou Q, Yang XQ, *et al*: Genistein alleviates radiation-induced pneumonitis by depressing Ape1/Ref-1 expression to down-regulate inflammatory cytokines. Cell Biochem Biophys 69: 725-733, 2014.
5. Wajant H, Pfizenmaier K and Scheurich P: Tumor necrosis factor signaling. Cell Death Differ 10: 45-65, 2003.
6. Javaid K, Rahman A, Anwar KN, Frey RS, Minshall RD and Malik AB: Tumor necrosis factor-alpha induces early-onset endothelial adhesivity by protein kinase Czeta-dependent activation of intercellular adhesion molecule-1. Circ Res 92: 1089-1097, 2003.
7. Sullivan DE, Ferris M, Pociask D and Brody AR: Tumor necrosis factor-alpha induces transforming growth factor-beta1 expression in lung fibroblasts through the extracellular signal-regulated kinase pathway. Am J Respir Cell Mol Biol 32: 342-349, 2005.
8. Chen Y, Williams J, Ding I, Hernady E, Liu W, Smudzin T, Finkelstein JN, Rubin P and Okunieff P: Radiation pneumonitis and early circulatory cytokine markers. Semin Radiat Oncol 12 (1 Suppl 1): S26-S33, 2002.
9. Hosoi Y, Miyachi H, Matsumoto Y, Enomoto A, Nakagawa K, Suzuki N and Ono T: Induction of interleukin-1beta and interleukin-6 mRNA by low doses of ionizing radiation in macrophages. Int J Cancer 96: 270-276, 2001.
10. Johnston CJ, Williams JP, Elder A, Hernady E and Finkelstein JN: Inflammatory cell recruitment following thoracic irradiation. Exp Lung Res 30: 369-382, 2004.
11. Hellweg CE: The Nuclear Factor kappaB pathway: A link to the immune system in the radiation response. Cancer Lett 368: 275-289, 2005.
12. Chishti AA, Baumstark-Khan C, Koch K, Kolanus W, Feles S, Konda B, Azhar A, Spitta LF, Henschenmacher B, Diegeler S, *et al*: Linear energy transfer modulates radiation-induced NF-kappa B activation and expression of its downstream target genes. Radiat Res 189: 354-370, 2018.
13. Pradere JP, Dapito DH and Schwabe RF: The Yin and Yang of Toll-like receptors in cancer. Oncogene 33: 3485-3495, 2014.
14. Yang K, Palm J, Konig J, Seeland U, Rosenkranz S, Feiden W, Rübe C and Rübe CE: Matrix-Metallo-Proteinases and their tissue inhibitors in radiation-induced lung injury. Int J Radiat Biol 83: 665-676, 2007.
15. Masamune A, Watanabe T, Kikuta K, Satoh K and Shimosegawa T: NADPH oxidase plays a crucial role in the activation of pancreatic stellate cells. Am J Physiol Gastrointest Liver Physiol 294: G99-G108,2008.
16. Stas S, Whaley-Connell A, Habibi J, Appesh L, Hayden MR, Karuparthi PR, Qazi M, Morris EM, Cooper SA, Link CD, *et al*: Mineralocorticoid receptor blockade attenuates chronic overexpression of the renin-angiotensin-aldosterone system stimulation of reduced nicotinamide adenine dinucleotide phosphate oxidase and cardiac remodeling. Endocrinology 148: 3773-3780, 2007.
17. Hecker L, Vittal R, Jones T, Jagirdar R, Luckhardt TR, Horowitz JC, Pennathur S, Martinez FJ and Thannickal VJ: NADPH oxidase-4 mediates myofibroblast activation and fibrogenic responses to lung injury. Nat Med 15: 1077-1081, 2009.
18. Rabbani ZN, Mi J, Zhang Y, Delong M, Jackson IL, Fleckenstein K, Salahuddin FK, Zhang X, Clary B, Anscher MS and Vujaskovic Z: Hypoxia inducible factor 1alpha signaling in fractionated radiation-induced lung injury: Role of oxidative stress and tissue hypoxia. Radiat Res 173: 165-174, 2010.
19. Mehta V: Radiation pneumonitis and pulmonary fibrosis in non-small-cell lung cancer: Pulmonary function, prediction, and prevention. Int J Radiat Oncol Biol Phys 63: 5-24, 2005.
20. Koopman FA, Schuurman PR, Vervoordeldonk MJ and Tak PP: Vagus nerve stimulation: A new bioelectronics approach to treat rheumatoid arthritis? Best Pract Res Clin Rheumatol 28: 625-635, 2014.
21. Kox M, Pompe JC, Peters E, Vaneker M, van der Laak JW, van der Hoeven JG, Scheffer GJ, Hoedemaekers CW and Pickkers P: α7 nicotinic acetylcholine receptor agonist GTS-21 attenuates ventilator-induced tumour necrosis factor-alpha production and lung injury. Br J Anaesth 107: 559-566, 2011.
22. Chatterjee PK, Yeboah MM, Dowling O, Xue X, Powell SR, Al-Abed Y and Metz CN: Nicotinic acetylcholine receptor agonists attenuate septic acute kidney injury in mice by suppressing inflammation and proteasome activity. PLoS One 7: e35361, 2012.
23. Sitapara RA, Antoine DJ, Sharma L, Patel VS, Ashby CR Jr, Gorasiya S, Yang H, Zur M and Mantell LL: The α7 nicotinic acetylcholine receptor agonist GTS-21 improves bacterial clearance in mice by restoring hyperoxia-compromised macrophage function. Mol Med 20: 238-247,2014.
24. World Medical Association General Assembly: Guiding principles for research involving animals and human beings. Am J Physiol Cell Physiol 280: 3p after R1913, 2002.
25. Chen J, Tian X, Mei Z, Wang Y, Yao Y, Zhang S, Li X, Wang H, Zhang J and Xie C: The effect of the TLR9 ligand CpG-oligodeoxynucleotide on the protective immune response to radiation-induced lung fibrosis in mice. Mol Immunol 80: 33-40, 2016.
26. Pavlov VA, Ochani M, Yang LH, Gallowitsch-Puerta M, Ochani K, Lin X, Levi J, Parrish WR, Rosas-Ballina M, Czura CJ, *et al*: Selective alpha7-nicotinic acetylcholine receptor agonist GTS-21 improves survival in murine endotoxemia and severe sepsis. Crit Care Med 35: 1139-44, 2007.
27. Giebelen IA, van Westerloo DJ, LaRosa GJ, de Vos AF and van der Poll T: Local stimulation of alpha7 cholinergic receptors inhibits LPS-induced TNF-alpha release in the mouse lung. Shock 28: 700-703, 2007.
28. Hübner RH, Gitter W, Mokhtari NE El, Mathiak M, Both M, Bolte H, Freitag-Wolf S and Bewig B: Standardized quantification of pulmonary fibrosis in histological samples. Biotechniques 44: 507-511, 2008.
29. Livak KJ and Schmittgen TD: Analysis of relative gene expression data using real-time quantitative PCR and the $2^{-\Delta\Delta CT}$ method. Methods 25: 402-408, 2001.
30. Freedman R, Olincy A, Buchanan RW, Harris JG, Gold JM, Johnson L, Allensworth D, Guzman-Bonilla A, Clement B, Ball MP, *et al*: Initial phase 2 trial of a nicotinic agonist in schizophrenia. Am J Psychiatry 165: 1040-1047, 2008.
31. Kitagawa H, Takenouchi T, Azuma R, Wesnes KA, Kramer WG, Clody DE and Burnett AL: Safety, pharmacokinetics, and effects on cognitive function of multiple doses of GTS-21 in healthy, male volunteers. Neuropsychopharmacology 28: 542-551, 2003.
32. Leib C, Goser S, Luthje D, Ottl R, Tretter T, Lasitschka F, Zittrich S, Pfitzer G, Katus HA and Kaya Z: Role of the cholinergic antiinflammatory pathway in murine autoimmune myocarditis. Circ Res 109: 130-140, 2011.
33. Saito-Fujita T, Iwakawa M, Nakamura E, Nakawatari M, Fujita H, Moritake T and Imai T: Attenuated lung fibrosis in interleukin 6 knock-out mice after C-ion irradiation to lung. J Radiat Res 52: 270-277, 2011.
34. Przybyszewska M, Miloszewska J, Rzonca S, Trembacz H, Pysniak K, Kotlarz A, Swoboda P, Zalewska M and Małecki M: Soluble TNF-α receptor I encoded on plasmid vector and its application in experimental gene therapy of radiation-induced lung fibrosis. Arch Immunol Ther Exp 59: 315-326, 2011.
35. Zhao DY, Qu HJ, Guo JM, Zhao HN, Yang YY, Zhang P, Cao K, Lei X, Cui JG, Liu C, *et al*: Protective effects of myrtol standardized against radiation-induced lung injury. Cell Physiol Biochem 38: 619-634, 2016.
36. Rübe CE, Wilfert F, Palm J, König J, Burdak-Rothkamm S, Liu L, Schuck A, Willich N and Rübe C: Irradiation induces a biphasic expression of pro-inflammatory cytokines in the lung. Strahlenther Onkol 180: 442-448,2004.
37. Haase MG, Klawitter A, Geyer P, Alheit H, Baumann M, Kriegel TM, Kasper M and Baretton GB: Sustained elevation of NF-kappaB DNA binding activity in radiation-induced lung damage in rats. Int J Radiat Biol 79: 863-877,2003.
38. Li F, Chen Z, Pan Q, Fu S, Lin F, Ren H, Han H, Billiar TR, Sun F and Li Q: The protective effect of PNU-282987, a selective alpha7 nicotinic acetylcholine receptor agonist, on the hepatic ischemia-reperfusion injury is associated with the inhibition of high-mobility group box 1 protein expression and nuclear factor kappaB activation in mice. Shock 39: 197-203, 2013.

39. Café-Mendes CC, Garay-Malpartida HM, Malta MB, de Sá Lima L, Scavone C, Ferreira ZS, Markus RP and Marcourakis T: Chronic nicotine treatment decreases LPS signaling through NF-κB and TLR-4 modulation in the hippocampus. Neurosci Lett 636: 218-224, 2017.
40. Anders HJ, Banas B and Schlondorff D: Signaling danger: Toll-like receptors and their potential roles in kidney disease. J Am Soc Nephrol 15: 854-867, 2004.
41. Yu M, Wang H, Ding A, Golenbock DT, Latz E, Czura CJ, Fenton MJ, Tracey KJ and Yang H: HMGB1 signals through toll-like receptor (TLR) 4 and TLR2. Shock 26: 174-179, 2006.
42. Rhieu BH, Epperly MW, Cao S, Goff J, Shields D, Franicola D, Wang H and Greenberger JS: Improved longevity of hematopoiesis in long-term bone marrow cultures and reduced irradiation-induced pulmonary fibrosis in Toll-like receptor-4 deletion recombinant-negative mice. In Vivo 28: 441-448, 2014.
43. Kox M, van Velzen JF, Pompe JC, Hoedemaekers CW, van der Hoeven JG, and Pickkers P: GTS-21 inhibits pro-inflammatory cytokine release independent of the Toll-like receptor stimulated via a transcriptional mechanism involving JAK2 activation. Biochem Pharmacol 78: 863-872, 2009.
44. Guijarro-Munoz I, Compte M, Alvarez-Cienfuegos A, Alvarez-Vallina L and Sanz L: Lipopolysaccharide activates Toll-like receptor 4 (TLR4)-mediated NF-kappaB signaling pathway and proinflammatory response in human pericytes. J Biol Chem 289: 2457-2468, 2014.
45. He ZW, Qin YH, Wang ZW, Chen Y, Shen Q and Dai SM: HMGB1 acts in synergy with lipopolysaccharide in activating rheumatoid synovial fibroblasts via p38 MAPK and NF-kappaB signaling pathways. Mediators Inflamm 2013: 596716, 2013.
46. Pusterla T, Nemeth J, Stein I, Wiechert L, Knigin D, Marhenke S, Longerich T, Kumar V, Arnold B, Vogel A, *et al*: Receptor for advanced glycation endproducts (RAGE) is a key regulator of oval cell activation and inflammation-associated liver carcinogenesis in mice. Hepatology 58: 363-373,2013.
47. Candeias SM and Testard I: The many interactions between the innate immune system and the response to radiation. Cancer Lett 368: 173-178 2015.
48. Menendez D, Shatz M, Azzam K, Garantziotis S, Fessler MB and Resnick MA: The Toll-like receptor gene family is integrated into human DNA damage and p53 networks. PLoS Genet 7: e1001360 2011.
49. Li X, Ma D, Zha X, Quan D, Pan D, Sun M, Hu B and Zhao B: Ilomastat, a synthetic inhibitor of MMPs, prevents lung injury induced by γ-ray irradiation in mice. Oncotarget 8: 60789-60808, 2017.
50. Hiramoto T, Chida Y, Sonoda J, Yoshihara K, Sudo N and Kubo C: The hepatic vagus nerve attenuates Fas-induced apoptosis in the mouse liver via alpha7 nicotinic acetylcholine receptor. Gastroenterology 134: 2122-2131, 2008.
51. Navarro E, Buendia I, Parada E, León R, Jansen-Duerr P, Pircher H, Egea J and Lopez MG: Alpha7 nicotinic receptor activation protects against oxidative stress via heme-oxygenase I induction. Biochem Pharmacol 97: 473-481, 2015.
52. Yahyapour R, Motevaseli E, Rezaeyan A, Abdollahi H, Farhood B, Cheki M, Rezapoor S, Shabeeb D, Musa AE, Najafi M and Villa V: Reduction-oxidation (redox) system in radiation-induced normal tissue injury: Molecular mechanisms and implications in radiation therapeutics. Clin Transl Oncol 20: 975-988, 2018.
53. Jenkins SJ, Ruckerl D, Cook PC, Jones LH, Finkelman FD, van Rooijen N, MacDonald AS and Allen JE: Local macrophage proliferation, rather than recruitment from the blood, is a signature of TH2 inflammation. Science.3 32: 1284-1288, 2011.
54. Han G, Zhang H, Xie CH and Zhou YF: Th2-like immune response in radiation-induced lung fibrosis. Oncol Rep 26: 383-388, 2011.
55. Mei ZJ, Chen J, Xie CH, *et al*: α7-nAchR Agonist GTS-21 Reduces Radiation-Induced Lung Injury by Inhibiting HMGB1/TLR-4/NF-κB Pathway. Topic: Biology, IASLC 17th World Conference, Vienna, 2016.